DOI: 10.1002/ejoc.200901275

Synthesis, NMR, and Conformational Studies of Cyclic Oligo-(1→6)-β-D-Glucosamines

Marina L. Gening,[a] Denis V. Titov,[a,b] Alexey A. Grachev,[a] Alexey G. Gerbst,[a] Olga N. Yudina,[a] Alexander S. Shashkov,[a] Alexander O. Chizhov,[a] Yury E. Tsvetkov,[a] and Nikolay E. Nifantiev*[a]

Dedicated to Professor Klaus Bock on the occasion of his 65th birthday

Keywords: Carbohydrates / Oligosaccharides / Conformation analysis / Macrocycles

The first synthesis of a series of homologous cyclic oligo-(1→6)-β-D-glucosamines consisting of two to seven residues and representing a new type of functionalized cyclic oligosaccharides is reported. Remarkably high yields of the studied macrocyclization reaction irrespective of the length of the acyclic precursors were observed. In the case of compounds constituted of four to seven glucosamine units α-stereoisomers formed as side products despite the presence of a strongly participating 2-*N*-phthaloyl group to control β-glycosylation. Both phenomena may be accounted for by conformational features of the linear bifunctional precursors. According to computer modeling and NMR conformational studies, the described linear (1→6)-β-linked oligoglucosamines exist in a right-handed helix-like conformation, in which the glycosyl donor and acceptor moieties are prearranged in a way that facilitates intramolecular glycosylation from the α-side. Prepared cyclo-oligoglucosamines differ in their conformational flexibilities, as illustrated by their spectral characteristics and calculated asphericity distributions. Moreover, the obtained compounds do not possess a distinct hydrophobic cavity, which is in contrast to the well-known cyclodextrins. All these characteristics provide an excellent basis for the use of these novel cyclic oligosaccharides as scaffolds for the construction of biomolecular conjugates.

Introduction

The synthesis of carbohydrate macrocycles is a challenging task.[1] In general, cyclizations to form large rings require the formation of a cyclic transition state from acyclic precursors that can adopt numerous conformations. The probability of attaining the cyclic transition state decreases dramatically with elongation of the linear chain. This results from significant loss of entropy due to coiling of the extended acyclic precursors. For example, the relative reaction rate for the formation of an eight-membered lactone is six orders of magnitude lower than that for a five-membered one.[2] Larger bifunctional precursors more readily undergo intermolecular condensation instead of macrocyclization, and therefore, high dilution or other special techniques are necessary for the effective formation of cyclic products.

[a] N. D. Zelinsky Institute of Organic Chemistry RAS
Leninsky prospect 47, 119991 Moscow, Russia
Fax: +7-499-135-87-84
E-mail: nen@ioc.ac.ru
[b] Higher Chemical College RAS
Miusskaya sq. 9, 125047 Moscow, Russia
Fax: +7-499-978-85-27
Supporting information for this article is available on the WWW under http://dx.doi.org/10.1002/ejoc.200901275.

The preparation of cyclo-oligosaccharides by intramolecular glycosylation of bifunctional oligosaccharide blocks is more complicated, as the number of available conformations is restricted due to specific properties of the glycoside linkage. As a result of the limited conformational space, the cyclization occurs efficiently only at a certain length of the linear oligosaccharide precursors. For instance, maltooligosaccharides are properly preorganized for ring closure when the number of D-glucopyranose units is six, seven, or eight.[1] This preorganization explains the efficiency of the enzymatic production of α-, β-, and γ-cyclodextrins. Another illustration is the chemical synthesis of cyclic (1→4)-α-D-mannopyranosides, where the observed yield for the macrocyclization of penta- and hexasaccharides was 8 and 92%, respectively.[3–5]

Despite considerable research activity in the field of synthetic cyclic oligosaccharides, there have been no examples to date of these compounds with D-glucosamine units and only a few discrete examples of cycles with (1→6)-glycoside linkages.[6–9] The work described here was initiated by our recent observation[10] that cyclization of bifunctional disaccharide **1** and trisaccharide **2** (Scheme 1) resulted in the almost quantitative formation of corresponding cyclic products **3** and **4**, and surprisingly, the formation of linear oligomers was not detected. This is in contrast with previous

examples of cyclo-oligomerization involving small oligosaccharide blocks.[11–15] Here we report on the cyclization of oligo-(1→6)-β-D-glucosamine derivatives containing up to seven monosaccharide units and the synthesis of the corresponding cyclic oligosaccharides. A variety of modern techniques was employed to reveal structural characteristics of all synthesized oligosaccharides and to study the conformational basis for the stereochemistry of cycloglycosylation.

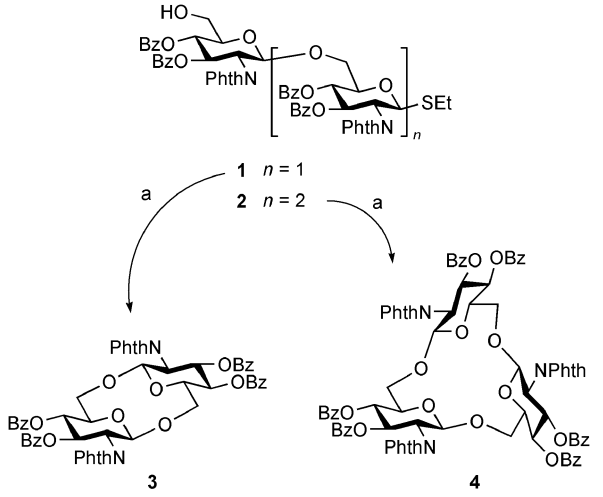

Scheme 1. Cyclization of oligosaccharides **1** and **2**. Reagents and conditions: (a) NIS, TfOH, CH_2Cl_2, 4 Å MS, –15 °C, 90–95%.

Results and Discussion

Synthesis of Cyclic Oligo-(1→6)-β-D-Glucosamines

A series of homologous bifunctional blocks **7**–**10** were used as the precursors of target cyclic oligoglucosamines. Compounds **7**–**10** were prepared by using a convergent approach (Scheme 2). Thus, disaccharide thioglycoside **5**[16] was converted into bromide **6**,[16] which was used as a key glycosylating agent for chain elongation. Its coupling with di- and trisaccharide glycosyl acceptors **1**[10] and **2**[10] and subsequent selective *O*-deacetylation produced corresponding thioglycosides **7** and **9** bearing a free OH group at the terminal "nonreducing" GlcN unit. Repetition of the same procedures with the obtained products afforded hexasaccharide **8** and heptasaccharide **10** in good yields.

Then, cyclization of bifunctional (1→6)-β-D-glucosamine oligomers **7**–**10** constituted of four to seven monosaccharide units was investigated. Regardless of the length of the linear precursor, *N*-iodosuccimide (NIS)-trifluoromethanesulfonic acid (TfOH) promoted activation of **7**–**10** afforded corresponding cyclic products **11**–**14** in good yields (Scheme 3). Practically no products of linear oligomerization were detected, even at concentrations up to 10 times higher than those described for the cyclization of other linear oligosaccharides.[6–9] Strong prevalence of intramolecular glycosylation over linear chain elongation may be explained by the conformational preorganization of the precursors in a shape providing spatial proximity of the terminal glycosyl donor and acceptor moieties. It was noticeable that the intramolecular glycosylation of compounds **7**, **8**, and **10** resulted in the formation of symmetric cycles **11β**, **13β**, and **14β** as major products along with minor amounts of (1→6)-α-linked cycles **11α**, **13α**, and **14α** (Scheme 3) which were obtained in individual state. Cyclization of **9** afforded **12β** almost exclusively; corresponding α-linked cycle **12α** apparently also formed, but its very low yield (<3%) did not allow its isolation and unambiguous characterization.

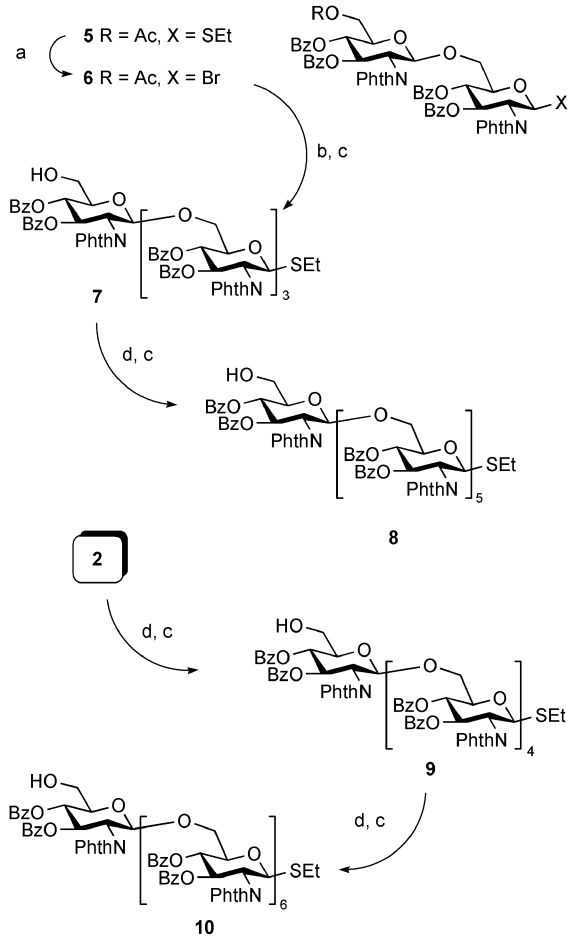

Scheme 2. Synthesis of linear precursors **7**–**10**. Reagents and conditions: (a) Br_2, CH_2Cl_2; (b) **1**, $HgBr_2$, $Hg(CN)_2$, MeCN, 3 Å MS; (c) HCl/MeOH; (d) **6**, $HgBr_2$, $Hg(CN)_2$, MeCN, 3 Å MS.

The structures of the β- and α-isomers of cyclic products **11**–**14** were deduced from their NMR and mass spectroscopic data. The NMR spectra of products **11β**–**14β** contained only the signals of one monosaccharide repeating unit due to their symmetry and confirmed that all glucosamine residues have the β-configuration. It was not possible to determine the anomeric configuration of the α-units in **11α**, **13α**, and **14α** from the corresponding $J_{1,2}$ values as a result of peak overlap in the ^1H NMR spectra. Their α-configuration was confirmed on the basis of a characteristic downfield shift of the signals for H-3, which appeared at 6.9–7.3 ppm. The cyclic nature of compounds **11α**, **13α**, and **14α** was confirmed by the presence of a correlation cross-

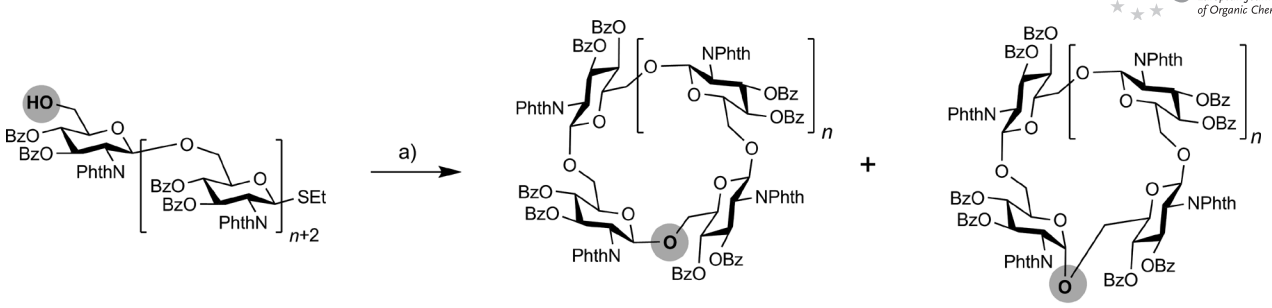

7 *n* = 1	**11**β (68%)	**11**α (17%)
9 *n* = 2	**12**β (81%)	**12**α
8 *n* = 3	**13**β (69%)	**13**α (11%)
10 *n* = 4	**14**β (59%)	**14**α (10%)

Scheme 3. Cyclization of oligosaccharides **7**–**10**. Reagents and conditions: (a) NIS, TfOH, CH_2Cl_2, 4 Å MS, –15 °C.

peak between H-1 of the α-residue with H-6 of another glucosamine residue in the ROESY spectra. The absence of the signals for non-glycosylated C-6 in the ^{13}C NMR spectra, which are typically observed in the range of 60–62 ppm, also supported the cyclic structure of these compounds.

Conformational Analysis of Linear Tetrasaccharide 7

The formation of the α-products upon the cyclization of bifunctional blocks **7**–**10** was unexpected because they contain a strongly participating *N*-phthaloyl blocking group at C-2 that provides stereospecific β-glycosylation, especially if a primary OH group is involved. To the best of our knowledge, only one example of α-glycoside bond formation upon glycosylation with the glycosyl donors having the participating *N*-phthaloyl group has been described so far without any explanation of the observed stereochemical outcome.[17] We supposed that the α-linked cycles formed as a result of conformational features of the linear precursors, which were illustrated by the example of tetrasaccharide **7**. The spatial structure of (1→6)-linked pyranosides (such as compound **7**) is primarily described by the dihedral angles ϕ, ψ, and ω around the bridges between the monosaccharide residues (Figure 1). Conformations of pyranoside rings change slightly and are considered to have little influence on the conformation of the whole saccharide molecule.[18] The values of these dihedral angles are related with the experimentally measured coupling constant values $J_{H,H}$ and $J_{C,H}$ around the glycosidic linkages through the Karplus equation[19,20] (Figure 1). Hence, we performed the analysis of the values of $J_{H,H}$ and $J_{C,H}$ calculated from molecular dynamics (MD) simulations and experimental ones. The experimental values of $^3J_{H,H}$ were measured from the ^1H NMR spectra and the values of long-range coupling constants $^3J_{C,H}$ were determined by employing 2D *J*-HMBC[21,22] NMR techniques. The detailed description of the NMR technique for the measurement of transglycosidic coupling constants in oligosaccharides is given in our previous work[23] and in the Experimental Section of this article. At the beginning, we obtained experimental values of transglycosidic constants for the molecule in CD_2Cl_2 solution at 268 K (Table 1) because these conditions are close to those used for cyclization of tetrasaccharide **7**. However, we could not determine in this case some constant values of interest (Table 1) due to the overlap of the signals. Therefore, the values of transglycosidic constants were additionally measured for compound **7** in $CDCl_3$ solution at 303 K (Table 2). The comparison of the constants for CD_2Cl_2 and $CDCl_3$ has shown that the corresponding values are close to each other (usually the difference does not exceed 1 Hz), thus revealing the conformational similarity of **7** in these two solvents.

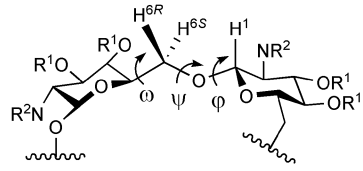

$$J\varphi = {}^3J_{C_6,H_1}$$
$$J\psi_R = {}^3J_{C_1,H_{6R}}$$
$$J\psi_S = {}^3J_{C_1,H_{6S}}$$
$$\Big\} \quad {}^3J_{C,H} = 5.5\cos^2\theta - 0.7\cos\theta + 0.6$$

$$J\omega_R = {}^3J_{H_{6R},H_5} = 5.08 + 0.47\cos\omega + 0.9\sin\omega - 0.12\cos(2\omega) + 4.86\sin(2\omega)$$

$$J\omega_S = {}^3J_{H_{6S},H_5} = 4.92 - 1.29\cos\omega + 0.05\sin\omega + 4.58\cos(2\omega) + 0.07\sin(2\omega)$$

Figure 1. Dihedral angles and the Karplus equations for the coupling constants $^3J_{C,H}$[19] and $^3J_{H,H}$[20] describing the conformation of the (1→6)-linkage.

Analysis of the conformers obtained from MD simulations for tetrasaccharide **7** shows that the conformations of the C1–O6 bonds are most rigid. For these bonds the typical values of the ϕ angles are in the range from +20° to +50°, which is in accordance with the exoanomeric effect. Rotation around the O6–C6 bond (angles ψ_R and ψ_S, Figure 1) results in two conformers with ψ_R and ψ_S angles of

Table 1. Experimental (CD_2Cl_2, 268 K) and calculated (in parentheses) values of transglycosidic ^3J coupling constants [Hz] for compound **7**.

Bond[a]	$J\phi$	$J\psi_R$	$J\psi_S$	$J_{H\text{-}5,H\text{-}6R}$	$J_{H\text{-}5,H\text{-}6S}$
B→A	2.5 (3.3)	nd[b] (2.5)	2.3 (2.6)	nd[b] (4.5)	2.0 (2.2)
C→B	2.5 (3.3)	nd[b] (2.9)	2.5 (2.4)	nd[b] (4.4)	2.9 (2.5)
D→C	3.3 (3.2)	nd[b] (2.5)	2.7 (2.5)	4.9 (4.6)	3.3 (2.5)

[a] Unit labels are shown in Scheme 4. [b] Not determined due to peak overlap.

Table 2. Experimental values of transglycosidic ^3J coupling constants [Hz] for compound **7** ($CDCl_3$, 303 K).

Bond[a]	$J\phi$	$J\psi_R$	$J\psi_S$	$J_{H\text{-}5,H\text{-}6R}$	$J_{H\text{-}5,H\text{-}6S}$
B→A	3.6	2.8	2.8	5.5	2.4
C→B	3.5	3.3	3.0	4.6	3.9
D→C	3.5	3.1	2.8	4.8	4.0

[a] Unit labels are shown in Scheme 4.

(–20°, 50°) and (–60°, 20°), respectively. Although transitions between these conformers slightly change the shape of the saccharide chain, the helical conformation is generally maintained. Unfolded conformers appear due to the rotation around the C6–C5 bond. Two main rotamers are observed for this bond with O5–C5–C6–O6 angles ω of about –60° and +60°, respectively; the latter rotamer is responsible for the occurrence of unfolded conformations (not shown). Experimentally observed coupling constants are presumably averages over the ensemble of all these conformers, as the observed experimental values of the pairs of $J_{H\text{-}5,H\text{-}6R}$/$J_{H\text{-}5,H\text{-}6S}$ constants cannot be attributed to a single conformation. Calculated average values of constants show acceptable[19] coincidence with experimental ones (Table 1), which also confirms that the studied tetrasaccharide generally has a helical shape, whereas unfolded conformers are present in minor quantity. Hence, compound **7** in its preferential conformation represents one turn of a right-handed spiral (Scheme 4), in which C-1 of the glycosylating unit (A) and 6-OH of the glycosyl acceptor residue (D) are spatially prearranged in a way favoring α-glycosylation (**I**) to give **11α**. However, the anchimeric participation of the phthaloyl group impedes the immediate formation of α-linked cycle **11α** and also stabilizes glycosyl cationic intermediate **II**, which becomes stable enough to survive until reorganization to conformation **III** favoring β-attack. The observed stereochemical outcome of the cyclization of tetrasaccharide **7** is apparently a result of the competition between these two processes. Similar conformational α-stereocontrol could be also expected for longer bifunctional blocks **8**–**10** in which the terminal residues are situated on adjacent turns of the right-handed helical structure. The spectra of protected saccharides **8**–**10** are rather complicated, and hence, the accurate measurement of coupling constants and, subsequently, the determination of torsion angles in them are impossible. On the other hand, the data obtained from molecular dynamics simulations suggest that the preferable orientation around the C5–C6 bond in the structures with the β(1→6)-glycoside linkage is characterized by ω angle values of –60°, thus leading to a helical shape of the molecules. Presumably, the conformational reorganization of oligosaccharides **8**–**10** to adopt a conformation suitable for the intramolecular glycosylation proceeds through inter-

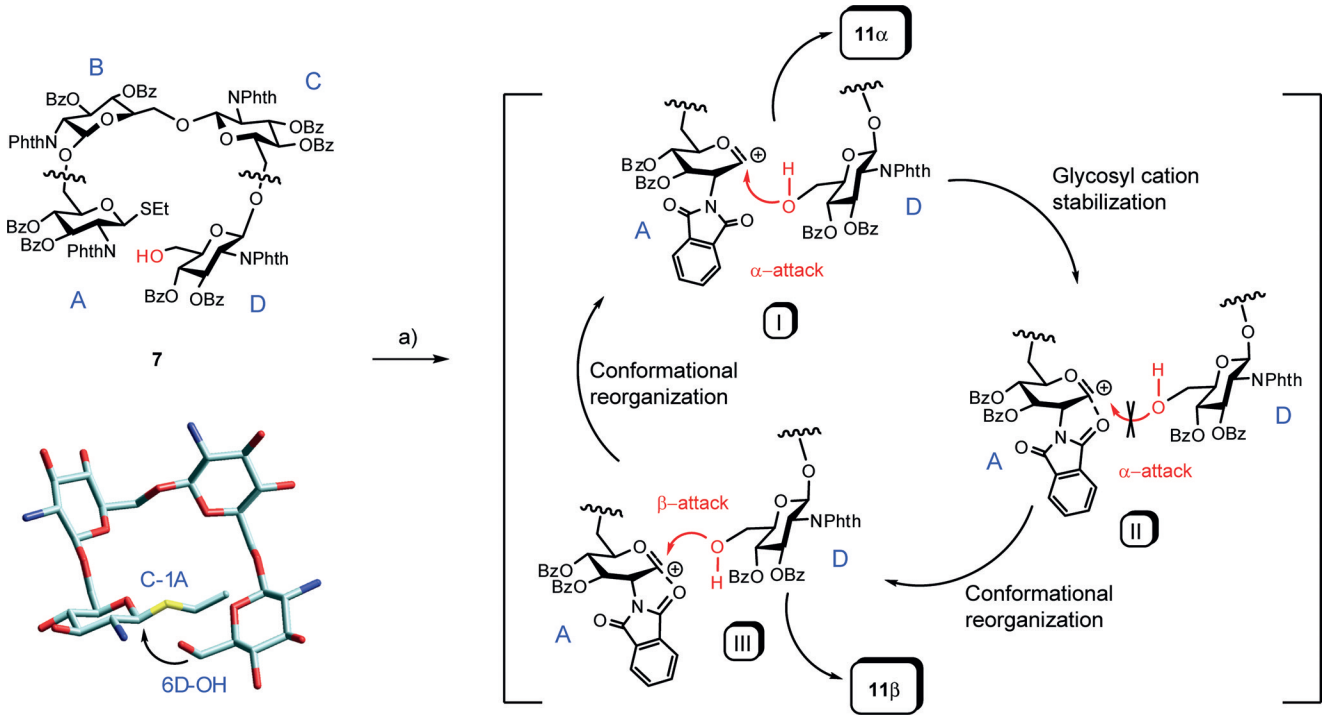

Scheme 4. Preferential conformation of tetrasaccharide **7** and possible intermediates explaining the stereochemical result of cyclization. Reagents and conditions: (a) NIS, TfOH, CH_2Cl_2, 4 Å MS, –15 °C.

mediate conformations, which also favor α-bond formation. The formation of α-linked cycles **11α**–**14α** can be regarded as a specific case of "tethered" glycosylation (for a recent review see ref.[24]).

Synthesis of Unprotected Cyclic Oligo-(1→6)-β-D-Glucosamines 15–26

The one-step deprotection of cyclic oligosaccharides by hydrazinolysis provided a series of free amines **15**–**20**, which were isolated as acetic acid salts. Further *N*-acetylation resulted in the formation of corresponding *N*-acetylated derivatives **21**–**26** (Figure 2). The structures of the thus obtained cyclic oligosaccharides were confirmed by mass spectrometry and ^{1}H and ^{13}C NMR spectroscopy (Tables 3 and 4, Figure 3). The NMR spectra were acquired at a temperature of 303–310 K. For each compound, the temperature was chosen so as to exclude the overlap of the solvent signal (HOD) with the anomeric proton signal of the cyclic glucosamines in the ^{1}H NMR spectrum.

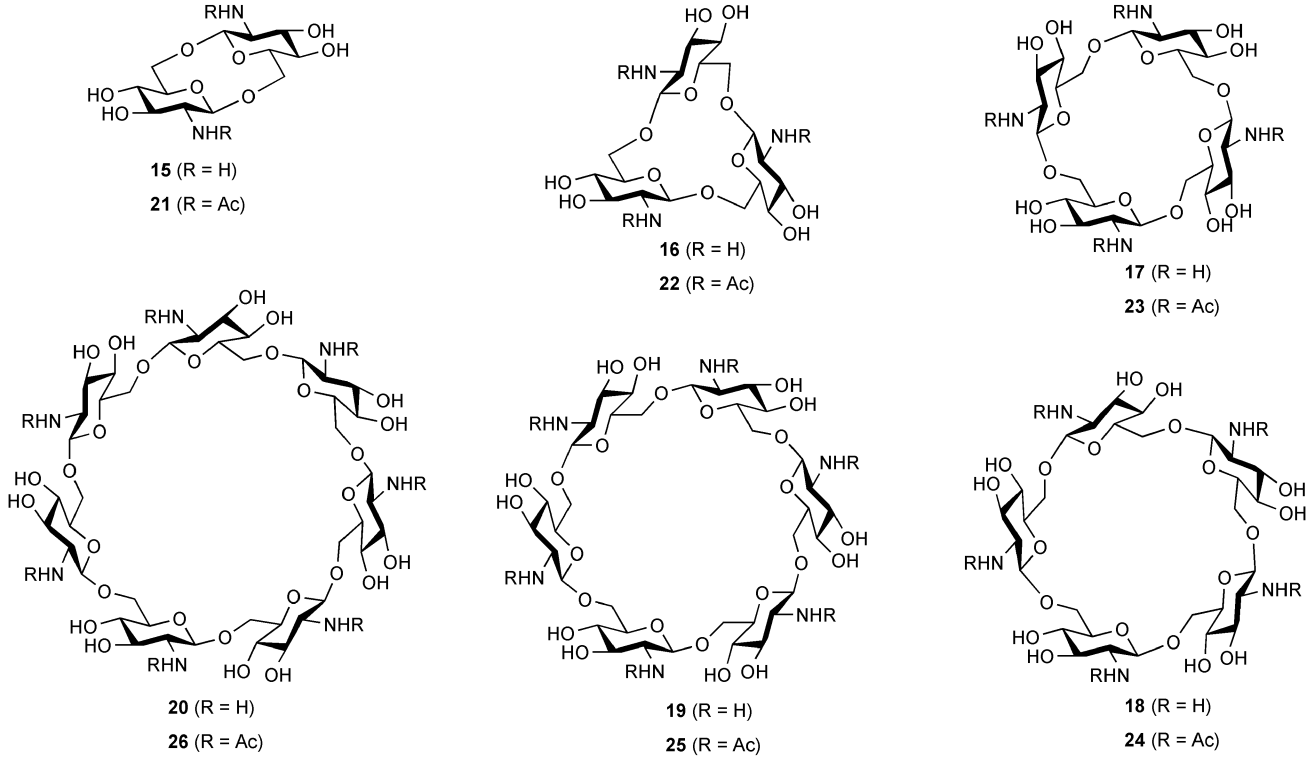

Figure 2. Final set of synthesized deprotected cyclic oligosaccharides. ^{1}H NMR spectra of compounds (a) **20** (303 K), (b) **19** (303 K), (c) **18** (310 K), (d) **17** (307 K), (e) **16** (307 K), and (f) **15** (303 K).

Table 3. ^{1}H NMR spectroscopic data for cyclic oligosaccharides **15**–**26** (D_2O, 500.13 or 600.13 MHz, 303–310 K).

	Chemical shift [δ, ppm]							Coupling constants [J, Hz]						
	H-1	H-2	H-3	H-4	H-5	H-6*R*	H-6*S*	1,2	2,3	3,4	4,5	5,6*R*	5,6*S*	6*R*,6*S*
15	4,95	3,33	3,72	4,17	3,85	4,12	3,73	≤2[b]	5.7	9.8	9.8	≤2.0[b]	≤2[b]	12.8
16	4.52	2.73	3.56	3.47	3.42	4.18	3.97	8.1	8.9	9.1	9.1	3.9	≤2[b]	12.2
17	4.74	3.03	3.67	3.72	3.60	4.07	4.14	8.5	8.8	9.2	9.5	2.5[	≤2[b]	11.0
18	4.74	3.04	3.65	3.58	3.61	4.03	4.13	8.4	8.7	10.2	9.4	4.0	≤2[b]	11.3
19	4.73	3.02	3.64	3.55	3.68	3.97	4.21	8.4	8.8	10.0	9.4	4.9	≤2[b]	11.5
20	4.79	3.06	3.67	3.60	3.66	3.96	4.20	8.4	9.0	9.1	9.1	3.7	≤2[b]	11.5
21	4.68	3.94	3.62	4.32	3.72	4.17	3.61	≤2[b]	5.7	9.9	9.9	≤2.0[b]	≤2[b]	12.8
22	4.60	3.64	3.49	3.46	3.48	4.09	3.90	8.4	9.6	nd[a]	nd[a]	4.1	≤2[b]	12.5
23	4.57	3.67	3.53	3.52	3.51	3.94	4.02	8.6	nd[a]	nd[a]	nd[a]	2.3	≤2[b]	11.4
24	4.59	3.67	3.55	3.46	3.53	3.90	4.07	8.3	10.1	9.0	9.4	4.9	≤2[b]	11.0
25	4.54	3.63	3.59	3.40	3.54	3.77	4.10	8.0	8.4	9.1	9.1	6.0	≤2[b]	11.1
26	4.58	3.70	3.57	3.47	3.57	3.82	4.13	8.4	8.6	9.2	9.4	5.2	≤2[b]	10.5

[a] Not determined due to peak overlap. [b] The small value of the coupling constant could not be measured exactly because of line broadening of the signals in the ^{1}H NMR spectra.

Table 4. ^{13}C NMR chemical shifts [δ, ppm] for cyclic oligosaccharides **15**–**26** (D_2O, 125.75 or 150.90 MHz, 303–310 K).

	C-1	C-2	C-3	C-4	C-5	C-6
15	100.1	60.1	71.8	67.6	79.4	70.0
16	102.4	57.4	75.7	70.5	76.0	69.3
17	100.2	56.6	73.1	69.8	75.7	69.4
18	100.9	56.9	73.4	70.6	76.2	69.8
19	100.8	56.8	73.5	70.8	75.7	69.5
20	100.8	56.8	73.2	70.8	75.9	69.5
21	103.3	59.9	74.3	67.9	78.1	71.3
22	101.4	57.0	75.2	70.6	75.8	69.7
23	102.3	56.7	75.0	70.5	75.9	69.5
24	102.8	56.8	74.8	71.0	76.2	69.9
25	102.6	56.9	74.7	71.3	75.7	70.2
26	102.7	56.8	74.9	71.3	75.9	69.8

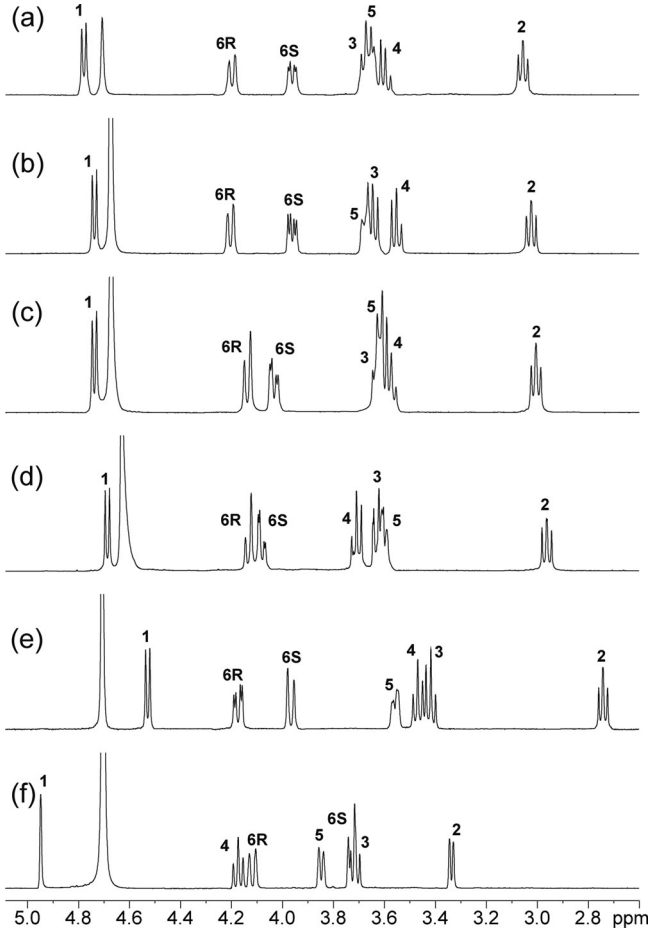

Figure 3. ^1H NMR spectra of compounds (a) **20** (303 K), (b) **19** (303 K), (c) **18** (310 K), (d) **17** (307 K), (e) **16** (307 K), and (f) **15** (303 K)..

NMR Spectroscopy and Theoretical Conformational Studies of Cyclic Oligo-(1→6)-β-D-glucosamines 15–26

The NMR spectra of all β-cycles contained the signals of one monosaccharide repeating unit, thus revealing the equivalence of all units within the cycle (Figure 3, Tables 3 and 4, and Supporting Information). Changes in the ^1H NMR spectra within the series of **15**–**20** and **21**–**26** reflect the changes in their conformational strain. Indeed, the increase in the cycle size from two to seven units is accompanied by changes in the localization of the signals and coupling constants values (Figure 3). It is also noticeable that in the case of disaccharides **15** and **21** the coupling constants $^3J_{H,H}$ within the glucosamine residues (Table 3) have atypical values for the glucopyranose in the $^4C_1$ conformation. This fact could be explained by conformational distortions of the pyranose rings in disaccharide cycles **15** and **21** due to steric hindrance. Similar distortion was already observed for cyclogentiobioside.[7,8]

To investigate the conformational properties of cyclic oligoglucosamines **15**–**26**, we performed analysis of the experimental values of transglycosidic constants $^3J_{H,H}$ and $^3J_{C,H}$ (Table 5). The experimental constants for small cycles changed significantly upon enlargement of the molecules. On the contrary, the constants for the cycles with five and more monosaccharide residues in the molecules coincided within the series of free oligoglucosamines **18**–**20** (in the form of ammonium salts) and the series of *N*-acetylated derivatives **24**–**26**. The spectral characteristics of these large cycles (Tables 3 and 4) are similar to those for internal units of the large linear oligoglucosamines described before.[16]

Table 5. Experimental transglycosidic coupling constants $^3J_{C,H}$ and $^3J_{H,H}$ [Hz] for cycles **15**–**26**.

	$J\phi$	$J\psi_R$	$J\psi_S$	$J_{H\text{-}5,H\text{-}6R}$	$J_{H\text{-}5,H\text{-}6S}$
15	4.3	2.2	6.0	≤2.0[a]	≤2[a]
16	3.8	3.2	5.2	3.9	≤2[a]
17	4.9	2.3	2.4	2.5	≤2[a]
18	3.8	2.7	2.8	4.0	≤2[a]
19	3.9	3.9	2.5	4.9	≤2[a]
20	3.8	3.5	3.2	3.7	≤2[a]
21	3.4	2.3	6.4	≤2.0[a]	≤2[a]
22	3.7	2.7	6.1	4.1	≤2[a]
23	4.9	2.5	3.5	2.3	≤2[a]
24	4.4	3.6	2.8	4.9	≤2[a]
25	3.5	3.7	2.4	6.0	≤2[a]
26	3.9	3.5	2.8	5.2	≤2[a]

[a] The small value of the coupling constant could not be measured exactly because of line broadening of the signals in the ^1H NMR spectra.

One of the main problems during the study of free oligoglucosamines **15**–**20** relates to the susceptibility of their ammonium salts to partial hydrolysis in water solution with the formation of free oligoglucosamines. We carried out molecular dynamics (MD) simulations for their fully protonated derivatives (NH_3^+ forms). Theoretical simulation of compounds **15**–**26** by using MD revealed that di-, tri-, and tetrasaccharides existed mostly in symmetrical ring-shaped conformations. Larger cycles tended to adopt more complicated shapes and the existence in conformations similar to that of **23** was unlikely for them. Row a in Figure 4 is composed of wireframe drawings that are superimpositions of different shape representatives found in MD trajectories for these molecules. It demonstrates the increasing flexibility of glycosidic linkages in the studied cycles upon their enlargement. After geometry optimizations of the structures generated during the MD simulations, global minima were found for each molecule. Those for saccharides containing four to

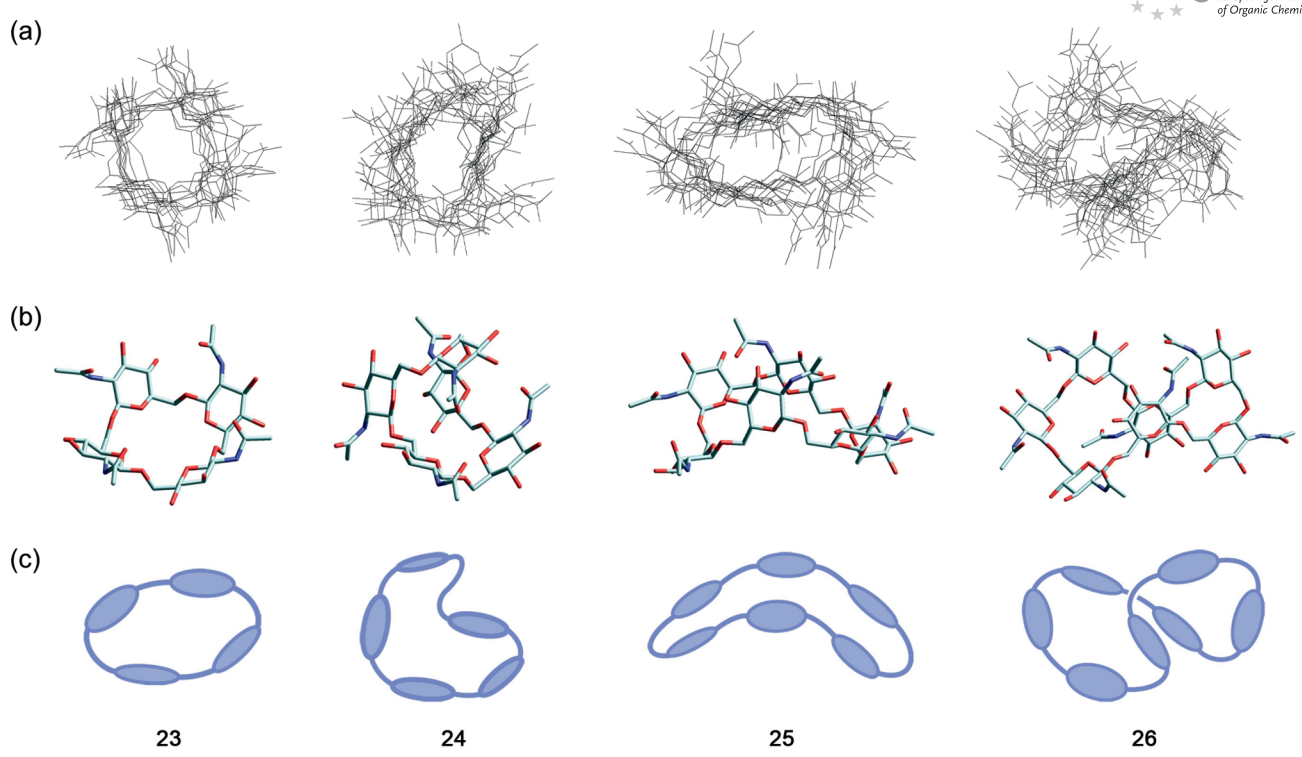

Figure 4. Superimpositions of eight different shapes found for cycles **23**–**26** during MD simulations (a); global minima for conformations of compounds **23**–**26** in the stick model (b) and schematic representations (c).

seven monosaccharide units are shown in Figure 4 (rows b and c) as a stick model and a schematic representation, respectively.

The asphericity parameters were calculated[25] for the conformations obtained from MD simulations. The formula used for the calculation of asphericity was $A^3/36\pi V^2$, where A is the molecule surface and V is the molecule volume. The higher value of this parameter indicates the greater deviation of the molecular shape from an "ideal sphere". As the areas under the curves are all normalized to the same value, the width of the distribution curve may be correlated to the number of conformational states available for the molecule. Thus, the broader curves are interpreted as showing a greater number of conformational states for the molecule. Figure 5 represents the asphericity distributions for oligoglucosamines **15**–**20** (ammonium salts) and their *N*-acetylated derivatives **21**–**26**, respectively. The disaccharides (both **15** and **21**) are unsurprisingly the most rigid ones; tri- and tetramers have moderate flexibilities, whereas cycles with a number of residues in the molecule of five and higher seem to adopt a wider range of possible conformations, which is reflected in the broadness of their asphericity distributions. In the case of cyclic penta-, hexa-, and heptasaccharides **18**–**20** and **24**–**26** (Figure 5), the distribution curves even look multicentered. This means that cycles with five and more residues in the molecule may undergo various conformational transformations like their linear counterparts. This conclusion is also supported by the results obtained from analysis of the coupling constant values, which showed that the conformational properties of the disaccharide fragments in cyclic penta-, hexa-, and heptasaccharides are similar and resemble those of long chain linear oligo-(1→6)-β-D-glucosamines.[16] It is also noteworthy that the distribution curves for oligoglucosamines **15**–**20** and corre-

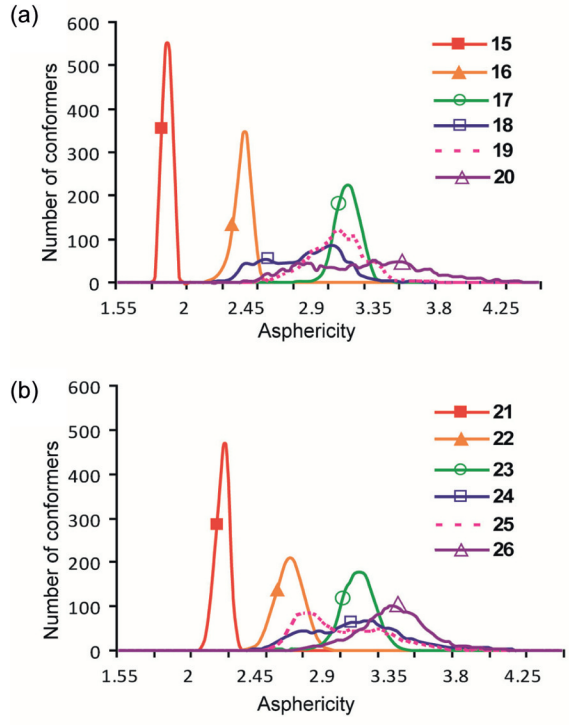

Figure 5. Asphericity distributions for (a) cyclic oligoglucosamines **15**–**20** (as ammonium acetate salts) and (b) oligo-*N*-acetylglucosamines **21**–**26**.

sponding *N*-acetylated derivatives **21**–**26** are similar to each other.

The calculation of the hydrophobicity and hydrophilicity distribution[26] exemplified by tetramer **23** (Figure 6) has shown that, unlike the well-known cyclodextrins, cyclo-oligo-(1→6)-β-D-glucosamines lack the distinct hydrophobic cavity.

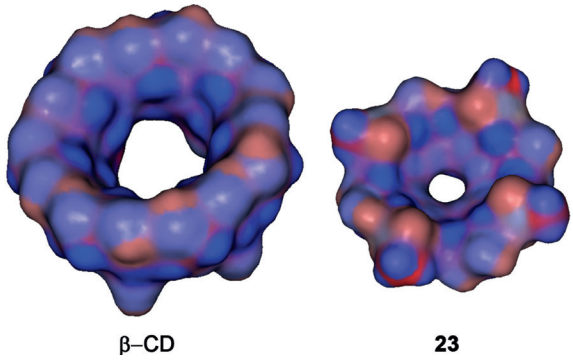

Figure 6. Distribution of the hydrophilic (red) and hydrophobic (blue) areas in molecules of tetrasaccharide **23** (outer diameter is 1.16 nm) and β-cyclodextrin (outer diameter is 1.44 nm).

Conclusions

In this paper we have discussed the remarkable ability of oligo-(1→6)-β-D-glucosamine derivatives **7**–**10** to undergo intramolecular glycosylation with the formation of a new family of functionalized cyclic oligosaccharides. As a result of their structure and molecular architectonics, these compounds may be regarded as convenient scaffolds for the design of conjugates with defined valency, symmetry, and flexibility. The absence of a distinct hydrophobic cavity precludes the possibility of the formation of inclusion complexes like in cyclodextrins. This may be an advantage for the use of described cyclo-oligoglucosamines as covalent carriers. Compounds **24**–**26** relate structurally to exopolysaccharide adhesin poly-(1→6)-β-D-glucosamine (PNAG) produced by *Staphylococcus aureus*,[27] *S. epidermidis*,[28] *Escherichia coli*,[29] *Bordetella bronchiseptica*,[30] *Actinobacillus pleuropneumoniae*,[31] and *Yersinia pestis*.[32] Thus, the obtained cyclo-oligosaccharides can be also regarded as potential inhibitors[33] of the biosynthesis of PNAG.

Experimental Section

General Information: NMR spectra were recorded with Bruker DRX-500 and Bruker Avance 600 instruments. Spectra of protected oligosaccharides were measured for solutions in $CDCl_3$, and ^1H NMR chemical shifts were referenced to the residual signal of $CHCl_3$. NMR spectra of free oligosaccharides were measured for solutions in D_2O by using acetone (δ_H = 2.225 ppm, δ_C = 31.45 ppm) as internal standard. HRMS (ESI) were obtained with Finnigan LTQ FT (Thermo Scientific) and MicrOTOF II (Bruker Daltonics) instruments. Optical rotations were measured by using a JASCO DIP-360 polarimeter at 18–22 °C in $CHCl_3$ in the case of the protected and partially protected derivatives and in water in the case of free oligosaccharides. TLC was performed on silica gel 60 F254 plates (E. Merck) and visualization was accomplished by using UV light or by charring with 10% H_3PO_4 in EtOH. Column chromatography was carried out on silica gel 60 (40–63 μm, E. Merck). Gel-permeation chromatography of protected oligosaccharides was performed with Bio-Beads SX-3 (13 × 450 mm) and Bio-Beads SX-1 (18 × 500) (Bio-Rad Laboratories) columns in toluene. Gel-permeation chromatography of free oligosaccharides was performed on a column of TSK HW-40 (S) gel (25 × 800 mm) in 0.1 M AcOH. All reactions involving air- or moisture-sensitive reagents were carried out by using dry solvents under an atmosphere of dry argon.

Special NMR Experiments: The values of long-range coupling constants $^3J_{C,H}$ were measured by employing a 2D *J*-HMBC[21,22] experiment, which was performed in the constant-time version.[21] The spectral widths were about 2.5 ppm for ^1H region and 50 ppm for ^{13}C region and did not include resonances of acetyl groups in the case of oligosaccharides **21**–**26**. The data were collected in the echo/antiecho mode. For echo selection the two sinusoidal field gradients in a ratio of 5:–3 are applied, and for antiecho selection the ratio was –3:5. The length of gradients was 1 ms, and the recovery time was 100 μs. The spectra were acquired with 60–100 t_1 increments and 40–500 scans per increment. A total of 512 points were collected during the acquisition time t_2. The HMBC preparation delay Δ for the reliable measurement of a coupling constants should be taken at least 60% of inversion values of smallest coupling of interest ($\Delta = 0.6/J_{C,H}^{min}$).[22] Smaller values of Δ lead to the overestimation of *J* because of the antiphase character of the peaks. Δ = 300 ms was used that corresponds to $J_{C,H}^{min}$ = 2.0 Hz. The upscaling coefficient *k* for determination of $^nJ_{C,H}$ from the spectra[21] was 30–60. The relaxation delay was 1 s. The third-order low-pass *J*-filter[22] was made on suppression of one bond constants ($^1J_{C,H}$) in the range from 125 Hz to 180 Hz. Sinusoidal field gradient sequence with the ratio +7:–4:–2:–1 was applied during low-pass *J*-filter. The forward linear prediction to 1024 points was used in F_1 that corresponds to resolution 5–6 Hz, and zero-filling to 1024 points was used in F_2. The processing was performed with π/2 shifted sine square function in both dimensions. The values of $^3J_{H,H}$ were measured from the ^1H NMR spectra.

Computer Simulations: MD simulations were carried out in vacuo with dielectric constant 81 by using MM3 force field (TINKER 4.1 program suit). Simulation time was 5 ns for each molecule. Snapshot structures were written every 5 ps and then used for further analysis. The geometry optimization of the snapshots led to 1000 structures among which the lowest energy conformer was chosen and used to represent the global minimum (Figure 4). In the case of linear protected precursor **7**, conformational search was first performed by using standard dihedral driving of ϕ and ψ angles. Two starting conformations were used; in the first one all ω angles were set to –60°, in the other to +60°. Two conformational maps were thus constructed for each glycosidic linkage with one local minimum found on each map. Six MD trajectories were then written, each starting from a different local minimum. *trans*-Glycosidic coupling constants were calculated for each structure of MD trajectories according to the Karplus equation and then averaged.

General Procedure A

Glycosylation Under Helferich Conditions: To a mixture of a glycosyl acceptor (0.1 mmol), $Hg(CN)_2$ (0.15 mmol), $HgBr_2$ (0.03 mmol), and 3 Å molecular sieves (500 mg) in anhydrous CH_3CN (3 mL) and CH_2Cl_2 (2 mL) was added a solution of a glycosyl bromide (0.15 mmol) in CH_3CN (2 mL) under an argon atmosphere. The reaction mixture was stirred for 30 min at room

temperature, diluted with CH_2Cl_2, and washed with 1 M aqueous KI, saturated aqueous $NaHCO_3$, and brine. The organic layer was dried with Na_2SO_4, filtered, and concentrated. The crude product was subjected to gel-chromatography in toluene, and the fractions with the highest molecular weight were collected and concentrated. Purification by silica gel column chromatography (toluene/EtOAc) afforded the corresponding coupling product.

General Procedure B

Selective *O*-Deacetylation in the Presence of Benzoates: A solution of the 6-*O*-acetyl derivative (0.1 mmol) in CH_2Cl_2 (2 mL) was diluted with absolute MeOH (2 mL) and then AcCl (0.1 mL, 1.4 mmol) was added under cooling with an ice bath. The mixture was kept for 16 h at room temperature and then concentrated. The residue was purified by silica gel column chromatography (EtOAc/toluene) to give the product with a free terminal 6-OH group.

General Procedure C

NIS/TfOH-Promoted Intramolecular Glycosylation–Cyclization: A mixture of the linear precursor (6 μmol), anhydrous dichloromethane (1 mL), and 4 Å molecular sieves (250 mg) was stirred under an argon atmosphere at room temperature. After 30 min, NIS (12 μmol) and TfOH (6 μmol) were added at –15 °C. The reaction mixture was stirred at –15 °C for an additional 30 min and then quenched with pyridine (5 μL), diluted with chloroform (20 mL), and filtered through a Celite layer. The filtrate was washed with 1 M aqueous $Na_2S_2O_3$, dried (Na_2SO_4), and concentrated. The crude product was purified by silica gel column chromatography (toluene/EtOAc) to give the cyclo-oligosaccharide. The molecular weight homogeneity and the absence of oligomerization products were established by gel-permeation chromatography of the crude products in toluene. The product was further purified either by silica gel column chromatography (toluene/EtOAc) or by C-18 reverse-phase chromatography (95% aq. CH_3CN).

Ethyl 3,4-Di-*O*-benzoyl-2-deoxy-2-phthalimido-β-D-glucopyranosyl-(1→6)-3,4-di-*O*-benzoyl-2-deoxy-2-phthalimido-β-D-glucopyranosyl-(1→6)-3,4-di-*O*-benzoyl-2-deoxy-2-phthalimido-β-D-glucopyranosyl-(1→6)-3,4-di-*O*-benzoyl-2-deoxy-2-phthalimido-1-thio-β-D-glucopyranoside (7): Following general procedure A, coupling of **3**[16] (101 mg, 0.095 mmol) and **6**[16] (152 mg, 0.14 mmol) followed by deacetylation according to general procedure B. Yield: 145 mg (74%). $[\alpha]_D^{20}$ = +8 (*c* = 1, $CHCl_3$). ^{1}H NMR (500 MHz, $CDCl_3$): δ = 7.95–7.15 (m, 56 H), 6.25 (t, *J* = 10.0 Hz, 1 H), 6.18 (t, *J* = 10.0 Hz, 1 H), 6.07 (m, 2 H), 5.60 (d, *J* = 8.4 Hz, 1 H), 5.51 (d, *J* = 10.5 Hz, 1 H), 5.43 (d, *J* = 8.4 Hz, 1 H), 5.39 (d, *J* = 8.4 Hz, 1 H), 5.34 (t, *J* = 9.7 Hz, 1 H), 5.28 (t, *J* = 9.6 Hz, 1 H), 5.22 (t, *J* = 9.6 Hz, 1 H), 5.18 (t, *J* = 9.6 Hz, 1 H), 4.50 (t, *J* = 10.4 Hz, 1 H), 4.43 (dd, *J* = 8.4, 10.5 Hz, 1 H), 4.33 (dd, *J* = 8.4, 10.5 Hz, 1 H), 4.25 (dd, *J* = 8.4, 10.5 Hz, 1 H), 4.03–3.97 (m, 2 H), 3.96–3.85 (m, 4 H), 3.82–3.76 (m, 3 H), 3.68–3.57 (m, 3 H) 5.05 (br. s, 1 H), 2.62 (m, 2 H), 1.15 (t, *J* = 8.5 Hz, 3 H) ppm. ^{13}C NMR (125 MHz, $CDCl_3$): δ = 167.0, 165.6, 165.5, 165.0, 164.9, 134.1, 134.0, 133.8, 133.2, 133.1, 131.6, 131.1, 129.8, 129.7, 129.1, 129.0, 128.7, 128.6, 128.3, 128.2, 125.2, 123.6, 98.04, 97.6, 97.5, 80.9, 77.2, 74.1, 72.6, 72.4, 72.0, 70.9, 70.6, 70.0, 69.8, 67.8, 67.5, 61.2, 54.7, 54.6, 53.8, 23.8, 15.0 ppm. $C_{114}H_{90}N_4O_{32}S$ (2060.01): calcd. C 66.47, H 4.40, N 2.72; found C 66.29, H 4.50, N 2.67.

Ethyl 3,4-Di-*O*-benzoyl-2-deoxy-2-phthalimido-β-D-glucopyranosyl-(1→6)-3,4-di-*O*-benzoyl-2-deoxy-2-phthalimido-β-D-glucopyranosyl-(1→6)-3,4-di-*O*-benzoyl-2-deoxy-2-phthalimido-β-D-glucopyranosyl-(1→6)-3,4-di-*O*-benzoyl-2-deoxy-2-phthalimido-β-D-glucopyranosyl-(1→6)-3,4-di-*O*-benzoyl-2-deoxy-2-phthalimido-1-thio-β-D-glucopyranoside (8): Following general procedure A, coupling of **7** (131 mg, 0.064 mmol) and **6**[16] (104 mg, 0.096 mmol) and subsequent deacetylation according to general procedure B. Yield: 104 mg (53%). $[\alpha]_D^{20}$ = +7 (*c* = 1, $CHCl_3$). ^{1}H NMR (500 MHz, $CDCl_3$): δ = 7.55–7.95 (m, 42 H), 7.12–7.51 (m, 42 H), 6.20 (t, *J* = 9.8 Hz, 1 H), 6.14 (t, *J* = 9.8 Hz, 1 H), 6.03–6.10 (m, 4 H), 5.55 (d, *J* = 8.1 Hz, 1 H), 5.47 (d, *J* = 10.4 Hz, 1 H), 5.30–5.5.44 (m, 4 H), 5.11–5.26 (m, 5 H), 5.05 (t, *J* = 8.4 Hz, 1 H), 4.48 (t, *J* = 10.4 Hz, 1 H), 4.41 (t, *J* = 8.6 Hz, 1 H), 4.19–4.31 (m, 4 H), 3.50–4.02 (m, 18 H), 2.65 (m, 2 H),1.11 (t, 3 H) ppm. ^{13}C NMR (125 MHz, $CDCl_3$): δ = 167.90, 167.12, 165.65, 165.56, 165.49, 165.17, 165.05, 164.86, 134.14, 133.86, 133.26, 131.10, 129.93, 129.74, 129.22, 129.11, 129.04, 128.73, 128.44, 128.22, 125.30, 123.59, 97.90 (C-1), 97.55 (C-1), 97.32 (C-1), 80.63 (C-1), 77.30, 74.16, 73.04, 72.74, 72.45, 72.28, 72.08, 70.99, 70.69, 70.31, 69.75, 67.98, 67.58, 67.03, 61.30 (C-6), 54.72, 54.60, 53.81, 23.71, 14.94 ppm. $C_{170}H_{132}N_6O_{48}S$ (3058.94): calcd. C 66.75, H 4.35, N 2.75; found C 66.68, H 4.29, N 2.75. HRMS (ESI): calcd. for $C_{170}H_{132}N_6O_{48}S$ [M + Na]$^+$ 3079.7690; found 3079.7685.

Ethyl 3,4-Di-*O*-benzoyl-2-deoxy-2-phthalimido-β-D-glucopyranosyl-(1→6)-3,4-di-*O*-benzoyl-2-deoxy-2-phthalimido-β-D-glucopyranosyl-(1→6)-3,4-di-*O*-benzoyl-2-deoxy-2-phthalimido-β-D-glucopyranosyl-(1→6)-3,4-di-*O*-benzoyl-2-deoxy-2-phthalimido-β-D-glucopyranosyl-(1→6)-3,4-di-*O*-benzoyl-2-deoxy-2-phthalimido-1-thio-β-D-glucopyranoside (9): Prepared from **4**[16] (106 mg, 0.069 mmol) and **6**[16] (108 mg, 0.1 mmol) according to general procedures A and B. Yield: 124 mg (70%). $[\alpha]_D^{20}$ = +5 (*c* = 1, $CHCl_3$). ^{1}H NMR (500 MHz, $CDCl_3$): δ = 7.61–7.95 (m, 35 H), 7.15–7.60 (m, 35 H), 6.00–6.27 (m, 5 H), 5.57 (d, *J* = 8.4 Hz, 1 H), 5.50 (d, *J* = 10.5 Hz, 1 H), 5.00–5.45 (m, 8 H), 4.40–4.55 (m, 3 H), 4.21–4.35 (m, 2 H), 3.53–4.05 (m, 12 H), 3.51–3.70 (m, 3 H), 3.05 (br. s, 1 H, O*H*), 2.62 (m, 2 H),1.10 (t, 3 H) ppm. ^{13}C NMR (125 MHz, $CDCl_3$): δ = 167.88, 167.11, 165.66, 165.54, 165.17, 164.93, 134.18, 133.85, 133.38, 133.26, 133.09, 131.64, 131.19, 129.95, 129.86, 129.74, 129.17, 129.10, 129.03, 128.92, 128.84, 128.72, 128.45, 128.37, 128.21, 125.30, 123.59, 97.85 (C-1), 97.47 (C-1), 97.32 (C-1), 80.62 (C^I-1), 77.27, 74.13, 72.95, 72.53, 72.20, 72.07, 70.95, 70.63, 70.39, 69.75, 67.90, 67.74, 67.62, 67.18, 61.25 (C^V-6), 54.70, 54.52, 53.80, 23.71, 14.95 ppm. $C_{142}H_{111}N_5O_{40}S$ (2559.48): calcd. C 66.64, H 4.37, N 2.74; found C 66.55, H 4.41, N 2.72. HRMS (ESI): calcd. for $C_{142}H_{111}N_5O_{40}S$ [M + Na]$^+$ 2580.6424; found 2580.6418.

Ethyl 3,4-Di-*O*-benzoyl-2-deoxy-2-phthalimido-β-D-glucopyranosyl-(1→6)-3,4-di-*O*-benzoyl-2-deoxy-2-phthalimido-β-D-glucopyranosyl-(1→6)-3,4-di-*O*-benzoyl-2-deoxy-2-phthalimido-β-D-glucopyranosyl-(1→6)-3,4-di-*O*-benzoyl-2-deoxy-2-phthalimido-β-D-glucopyranosyl-(1→6)-3,4-di-*O*-benzoyl-2-deoxy-2-phthalimido-β-D-glucopyranosyl-(1→6)-3,4-di-*O*-benzoyl-2-deoxy-2-phthalimido-1-thio-β-D-glucopyranoside (10): Prepared from **9** (223 mg, 0.087 mmol) and **6**[16] (94 mg, 0.131 mmol) according to general procedures A and B. Yield: 140 mg (45%). $[\alpha]_D^{20}$ = +10 (*c* = 1, $CHCl_3$). ^{1}H NMR (500 MHz, $CDCl_3$): δ = 7.57–8.05 (m, 49 H, Ar), 7.13–7.56 (m, 49 H, Ar), 6.05–6.30 (m, 7 H), 5.35–5.62 (m, 8 H), 5.05–5.33 (m, 6 H), 4.43–4.60 (m, 6 H), 4.18–4.40 (m, 8 H), 3.53–4.10 (m, 14 H), 3.23 (br. s, 1 H, O*H*), 2.62 (m, 2 H),1.10 (t, 3 H) ppm. ^{13}C NMR (125 MHz, $CDCl_3$): δ = 165.65, 165.56, 165.27, 165.13, 165.08, 164.96, 137.91, 134.20, 133.94, 133.31, 133.17, 131.71, 131.26, 130.00, 129.80, 129.12, 128.86, 128.80, 128.46, 128.29, 125.37, 123.64, 98.01 (C-1), 97.55 (C-1), 97.35 (C-1), 80.71 (C-1), 77.37, 74.20, 73.15, 72.89, 72.75, 72.61, 72.29, 72.15, 71.07, 70.72, 70.35, 70.24, 69.81, 67.98, 67.58, 67.21, 61.30 (C-6), 54.80, 53.86, 29.77, 23.69 (S*C*H$_2$CH$_3$), 14.93 (SCH$_2$*C*H$_3$) ppm. $C_{198}H_{153}N_7O_{56}S$ (3558.41): calcd. C 66.83, H 4.33, N 2.76; found C 66.75, H 4.37,

N 2.74. HRMS (ESI): calcd. for $C_{198}H_{153}N_7O_{56}S$ [M + Na]$^+$ 3578.8958; found 3578.8953.

Cyclotetrakis-(1→6)-(3,4-di-*O*-benzoyl-2-deoxy-2-phthalimido-β-D-glucopyranosyl) (11β) and (11α): Cyclization of **7** (187 mg, 0.082 mmol) according to general procedure C afforded **11β** (112 mg, 68%) and **11α** (28 mg, 17%). Ratio β/α = 4:1. Data for **11β**: Colorless foam. $[\alpha]_D^{20}$ = +3 (*c* = 1, $CHCl_3$). ^{1}H NMR (500 MHz, $CDCl_3$): δ = 7.71 (m, 4 H), 7.58 (m, 4 H), 7.37 (m, 2 H), 7.22 (m, 4 H), 6.09 (t, $J_{3,2}$ = $J_{3,4}$ = 9.5 Hz, 1 H, H-3), 5.77 (d, $J_{1,2}$ = 8.4 Hz, 1 H, H-1), 5.57 (t, $J_{4,5}$ = 9.4 Hz, 1 H, H-4), 4.71 (dd, 1 H, H-2), 4.16–4.02 (m, 3 H, H-5, 2 H-6) ppm. ^{13}C NMR (125 MHz, $CDCl_3$): δ = 167.9, 165.6, 164.6, 133.7, 132.9, 132.8, 131.7, 129.8, 129.6, 129.0, 128.7, 123.3, 98.3 (C-1), 74.6 (C-5), 71.6 (C-3), 69.6 (C-4), 68.5 (C-6), 54.3 (C-2) ppm. HRMS (ESI): calcd. for $C_{112}H_{84}N_4O_{32}$ [M + Na]$^+$ 2019.4966; found 2019.4961. Data for **11α**: Colorless foam. $[\alpha]_D^{20}$ = +29 (*c* = 0.5, $CHCl_3$). ^{1}H NMR (500 MHz, $CDCl_3$): δ = 7.98–7.20 (m, 56 H), 6.86 (br. t, *J* = 10.0 Hz, 1 H, H-3$^\alpha$), 6.33 (t, *J* = 10.0 Hz, 1 H), 6.25 (t, *J* = 10.0 Hz, 1 H), 5.99 (t, *J* = 10.4 Hz, 1 H), 5.85 (t, *J* = 10.4 Hz, 1 H), 5.71 (d, *J* = 8.5 Hz, 1 H), 5.62 (m, 2 H), 5.50 (t, *J* = 9.6 Hz, 1 H), 5.33 (m, 2 H), 5.01 (br. s, 1 H, H-1$^\alpha$), 4.88 (br. t, *J* = 9.6 Hz, 1 H), 4.82–4.77 (m, 2 H), 4.68–4.62 (m, 2 H), 4.26–4.20 (m, 2 H), 4.17 (m, 2 H), 4.00 (m, 1 H), 3.96–3.89 (m, 3 H), 3.87–3.82 (m, 2 H), 3.73 (m, 1 H) ppm. ^{13}C NMR (125 MHz, $CDCl_3$): δ = 165.6, 165.46, 164.0, 134.0, 133.7, 133.6, 133.4, 133.1, 132.9, 132.7, 132.6, 131.8, 131.7, 131.4, 130.1, 129.8, 129.7, 129.4, 129.3, 129.1, 128.9, 128.4, 128.2, 128.1, 127.9, 123.6, 98.8, 98.2, 97.8, 97.5, 73.65, 73.36, 73.19, 71.58, 71.16, 70.8, 70.2, 69.3, 67.9, 67.6, 65.9, 54.6, 54.2, 53.9 ppm. HRMS (ESI): calcd. for $C_{112}H_{84}N_4O_{32}$ [M + Na]$^+$ 2019.4966; found 2019.4961.

Cyclopentakis-(1→6)-(3,4-di-*O*-benzoyl-2-deoxy-2-phthalimido-β-D-glucopyranosyl) (12): Cyclization of **9** (96 mg, 0.038 mmol) according to general procedure C gave pure **12β** (59 mg, 63%) and an inseparable mixture of **12β/12α** (20 mg, 21%) in a ratio of ≈6:1 (^{1}H NMR spectra estimation). Data for **12β**: Colorless foam. $[\alpha]_D^{20}$ = +58 (*c* = 1, $CHCl_3$). ^{1}H NMR (600 MHz, $CDCl_3$): δ = 7.75 (m, 4 H), 7.62 (m, 4 H), 7.42 (m, 1 H), 7.38 (m, 1 H), 7.25 (m, 2 H), 7.19 (m, 2 H), 6.19 (t, $J_{3,2}$ = $J_{3,4}$ = 9.9 Hz, 1 H, H-3), 5.62 (t, $J_{4,5}$ = 9.6 Hz, 1 H, H-4), 5.57 (d, $J_{1,2}$ = 8.3 Hz, 1 H, H-1), 4.69 (dd, 1 H, H-2), 4.15 (d, $J_{6a,6b}$ = 9.1 Hz, 1 H, H-6a), 3.97 (m, 1 H, H-5), 3.87 (dd, $J_{6b,5}$ = 5.2 Hz, 1 H, H-6b) ppm. ^{13}C NMR (150 MHz, $CDCl_3$): δ = 167.8, 164.8, 133.7, 132.9, 132.8, 131.7, 129.8, 129.7, 129.2, 128.2, 128.1, 123.5, 97.9 (C-1), 72.9 (C-5), 71.4 (C-3), 70.5 (C-4), 68.0 (C-6), 54.7 (C-2) ppm. HRMS (ESI): calcd. for $C_{140}H_{105}N_5O_{40}$ [M + Na]$^+$ 2518.6233; found 2518.6228.

Cyclohexakis-(1→6)-(3,4-di-*O*-benzoyl-2-deoxy-2-phthalimido-β-D-glucopyranosyl) (13): Cyclization of **8** (72 mg, 0.023 mmol) according to general procedure C produced **13β** (48 mg, 69%) and **13α** (8 mg, 11%). Data for **13β**: Colorless foam. $[\alpha]_D^{20}$ = +36 (*c* = 1, $CHCl_3$). ^{1}H NMR (600 MHz, $CDCl_3$): δ = 7.75 (m, 4 H), 7.62 (m, 4 H), 7.42 (m, 1 H), 7.38 (m, 1 H), 7.25 (m, 2 H), 7.19 (m, 2 H), 6.25 (t, $J_{3,2}$ = $J_{3,4}$ = 9.9 Hz, 1 H, H-3), 5.61 (d, $J_{1,2}$ = 7.9 Hz, 1 H, H-1), 5.54 (br. t, $J_{4,5}$ = 9.1 Hz, 1 H, H-4), 4.69 (br. t, 1 H, H-2), 4.11 (d, $J_{6a,6b}$ = 10.0 Hz, 1 H, H-6a), 4.02 (br. m, 1 H, H-5), 3.95 (br. m, 1 H, H-6b) ppm. ^{13}C NMR (150 MHz, $CDCl_3$): δ = 165.6, 164.8, 133.7, 132.9, 132.8, 131.7, 129.8, 129.7, 129.2, 128.2, 128.1, 123.5, 97.5 (C-1), 73.2 (C-5), 71.4 (C-3), 70.5 (C-4), 66.8 (C-6), 54.6 (C-2) ppm. HRMS (ESI): calcd. for $C_{168}H_{126}N_6O_{48}$ [M + Na]$^+$ 3017.7500; found 3017.7495. Data for **13α**: Colorless foam. ^{1}H NMR (600 MHz, $CDCl_3$) selected signals: δ = 7.28 (H-3 α-GlcN), 5.64 (t, $J_{4,3}$ = $J_{4,5}$ = 9.5 Hz, 1 H, H-4 α-GlcN), 5.30–5.33 (br. m, 2 H, H-1 and H-2 α-GlcN), 4.27 (H-5 α-GlcN) ppm. HRMS (ESI): calcd. for $C_{168}H_{126}N_6O_{48}$ [M + Na]$^+$ 3017.7500; found 3017.7495.

Cycloheptakis-(1→6)-(3,4-di-*O*-benzoyl-2-deoxy-2-phthalimido-β-D-glucopyranosyl) (14): Cyclization of **10** (66 mg, 0.018mmol) according to general procedure C afforded **14β** (39 mg, 59%) and **14α** (8 mg, 10%). Ratio β/α ≈ 6:1. Data for **14β**: Colorless foam. $[\alpha]_D^{20}$ = +30 (*c* = 1, $CHCl_3$). ^{1}H NMR (600 MHz, $CDCl_3$): δ = 7.75 (m, 4 H), 7.62 (m, 4 H), 7.42 (m, 1 H), 7.38 (m, 1 H), 7.25 (m, 2 H), 7.19 (m, 2 H), 6.18 (t, $J_{3,2}$ = $J_{3,4}$ = 9.8 Hz, 1 H, H-3), 5.53 (d, $J_{1,2}$ = 8.3 Hz, 1 H, H-1), 5.46 (t, $J_{4,5}$ = 9.6 Hz, 1 H, H-4), 4.59 (dd, 1 H, H-2), 4.18 (d, $J_{6a,6b}$ = 9.8 Hz, 1 H, H-6a), 4.03 (m, 1 H, H-5), 3.89 (dd, $J_{6b,5}$ = 5.0 Hz, 1 H, H-6b) ppm. ^{13}C NMR (150 MHz, $CDCl_3$): δ = 167.8, 164.8, 133.7, 132.9, 132.8, 131.7, 129.8, 129.7, 129.2, 128.2, 128.1, 123.5, 97.8 (C-1), 73.4 (C-5), 71.4 (C-3), 70.1 (C-4), 67.1 (C-6), 54.6 (C-2) ppm. HRMS (ESI): calcd. for $C_{196}H_{147}N_7O_{56}$ [M + Na]$^+$ 3516.8767; found 3516.8762. Data for **14α**: ^{1}H NMR (600 MHz, $CDCl_3$) selected signals: δ = 7.17 (H-3 α-GlcN), 5.45 (H-4 α-GlcN), 5.19 (H-1 α-GlcN) 4.82 (dd, $J_{2,1}$ = 2.8 Hz, $J_{2,3}$ = 11.1 Hz, 1 H, H-2 α-GlcN), 4.45 (H-5 α-GlcN) ppm. HRMS (ESI): calcd. for $C_{196}H_{147}N_7O_{56}$ [M + 2Na]$^{2+}$ 1769.9327; found 1769.9327.

Cyclobis-(1→6)-(2-amino-2-deoxy-2-β-D-glucopyranosyl) (15): Prepared from **3**[16] (49 mg, 0.049 mmol) according to the published procedure for total deprotection.[16] Yield: 15 mg (95%). $[\alpha]_D^{20}$ = –22 (*c* = 1, H_2O). HRMS (ESI): calcd. for $C_{12}H_{22}N_2O_8$ [M + H]$^+$ 323.1449; found 323.1447.

Cyclotris-(1→6)-(2-amino-2-deoxy-2-β-D-glucopyranosyl) (16): Prepared from **4**[16] (39 mg, 0.026 mmol) according to the published procedure for total deprotection.[16] Yield: 12 mg (95%). $[\alpha]_D^{20}$ = –0.5 (*c* = 1, H_2O). HRMS (ESI): calcd. for $C_{18}H_{33}N_3O_{12}$ [M + H]$^+$ 484.2137; found 484.2136.

Cyclotetrakis-(1→6)-(2-amino-2-deoxy-2-β-D-glucopyranosyl) (17): Prepared from **11β** (65.8 mg, 0.033 mmol) according to the published procedure for total deprotection.[16] Yield: 20 mg (94%). $[\alpha]_D^{20}$ = –30 (*c* = 1, H_2O). HRMS (ESI): calcd. for $C_{24}H_{44}N_4O_{16}$ [M + H]$^+$ 645.2825; found 645.2826.

Cyclopentakis-(1→6)-(2-amino-2-deoxy-2-β-D-glucopyranosyl) (18): Prepared from **12β** (44.9 mg, 0.018 mmol) according the published procedure for total deprotection.[16] Yield: 14 mg (95%). $[\alpha]_D^{20}$ = –22 (*c* = 1, H_2O). HRMS (ESI): calcd. for $C_{30}H_{55}N_5O_{20}$ [M + H]$^+$ 806.3513; found 806.3510.

Cyclohexakis-(1→6)-(2-amino-2-deoxy-2-β-D-glucopyranosyl) (19): Prepared from **13β** (39 mg, 0.013 mmol) according to the published procedure for total deprotection.[16] Yield: 12 mg (96%). $[\alpha]_D^{20}$ = –14 (*c* = 1, H_2O). HRMS (ESI): calcd. for $C_{36}H_{66}N_6O_{24}$ [M + 2H]$^{2+}$ 484.2137; found 484.2135.

Cycloheptakis-(1→6)-(2-amino-2-deoxy-2-β-D-glucopyranosyl) (20): Prepared from **14β** (121 mg, 0.035 mmol) according to the published procedure for total deprotection.[16] Yield: 18 mg (92%). $[\alpha]_D^{20}$ = –12 (*c* = 1, H_2O). HRMS (ESI): calcd. for $C_{42}H_{77}N_7O_{28}$ [M + 2H]$^{2+}$ 564.7481; found 564.7479.

Cyclobis-(1→6)-(2-acetamido-2-deoxy-2-β-D-glucopyranosyl) (21): Prepared from **15** (5.7 mg, 0.0176 mmol) according to the published procedure for *N*-acetylation.[16] Yield: 7 mg (98%). $[\alpha]_D^{20}$ = +29 (*c* = 0.5, H_2O). HRMS (ESI): calcd. for $C_{16}H_{26}N_2O_{10}$ [M + Na]$^+$ 407.1480; found 407.1481.

Cyclotris-(1→6)-(2-acetamido-2-deoxy-2-β-D-glucopyranosyl) (22): Prepared from **16** (4.9 mg, 0.01 mmol) according to the published procedure for *N*-acetylation.[16] Yield: 6 mg (97%). $[\alpha]_D^{20}$ = –9 (*c* = 0.5, H_2O). HRMS (ESI): calcd. for $C_{24}H_{39}N_3O_{15}$ [M + Na]$^+$ 632.2273; found 632.2274.

Cyclotetrakis-(1→6)-(2-acetamido-2-deoxy-2-β-D-glucopyranosyl) (23): Prepared from **17** (8.7 mg, 0.012 mmol) according to the published procedure for *N*-acetylation.[16] Yield: 10 mg (98%). $[\alpha]_D^{20}$ = –9 (*c* = 1, H_2O). HRMS (ESI): calcd. for $C_{32}H_{52}N_4O_{20}$ $[M + H]^+$ 813.3248; found 813.3246.

Cyclopentakis-(1→6)-(2-acetamido-2-deoxy-2-β-D-glucopyranosyl) (24): Prepared from **18** (4.9 mg, 0.0061 mmol) according to the published procedure for *N*-acetylation.[16] Yield: 6 mg (97%). $[\alpha]_D^{20}$ = –10 (*c* = 1, H_2O). HRMS (ESI): calcd. for $C_{40}H_{65}N_5O_{25}$ $[M + H]^+$ 1016.4041; found 1016.4029.

Cyclohexakis-(1→6)-(2-acetamido-2-deoxy-2-β-D-glucopyranosyl) (25): Prepared from **19** (4.9 mg, 0.0051 mmol) according to the published procedure for *N*-acetylation.[16] Yield: 6 mg (97%). $[\alpha]_D^{20}$ = –22 (*c* = 1, H_2O). HRMS (ESI): calcd. for $C_{48}H_{78}N_6O_{30}$ $[M + Na]^+$ 1241.4655; found 1241.4660.

Cycloheptakis-(1→6)-(2-acetamido-2-deoxy-2-β-D-glucopyranosyl) (26): Prepared from **20** (6.5 mg, 0.0057 mmol) according to the general procedure for *N*-acetylation.[16] Yield: 8 mg (98%). $[\alpha]_D^{20}$ = –22 (*c* = 1, H_2O). HRMS (ESI): calcd. for $C_{56}H_{91}N_7O_{35}$ $[M + H]^+$ 1422.5629; found 1422.5633.

Supporting Information (see footnote on the first page of this article): Copies of the NMR spectra for all new compounds.

Acknowledgments

We are grateful for the financial support of the Russian Foundation for Basic Research (project no. 07-03-00603), and we acknowledge a grant from the President of the Russian Federation to Young Scientists (MK-5970.2008.3 to A.A.G.). We thank Professor G. B. Pier (Channing Laboratory, Brigham and Women's Hospital, Harvard Medical School, Boston, MA) for stimulating discussions.

[1] G. G. Gattuso, S. A. Nepogodiev, J. F. Stoddart, *Chem. Rev.* **1998**, *98*, 1919–1958.
[2] W. A. Smit, A. F. Bochkov, R. Caple (Eds.), *Organic Synthesis: The Science Behind the Art*, The Royal Society of Chemistry, Cambridge, **1998**, pp. 173–177.
[3] M. Mori, Y. Ito, T. Ogawa, *Tetrahedron Lett.* **1989**, *30*, 1273–1276.
[4] M. Mori, Y. Ito, T. Ogawa, *Carbohydr. Res.* **1989**, *192*, 131–146.
[5] M. Mori, Y. Ito, J. Uzawa, T. Ogawa, *Tetrahedron Lett.* **1990**, *31*, 3191–3194.
[6] N. K. Kochetkov, S. A. Nepogod′ev, L. V. Backinowsky, *Tetrahedron* **1990**, *46*, 139–150.
[7] D. Gagnaire, V. Tran, M. Vignon, *J. Chem. Soc., Chem. Commun.* **1976**, 6–7.
[8] D. Gagnaire, M. Vignon, *Carbohydr. Res.* **1976**, *51*, 140–144.
[9] S. Houdier, P. J. A. Vottero, *Angew. Chem.* **1994**, *106*, 365–367; *Angew. Chem. Int. Ed. Engl.* **1994**, *33*, 354–356.
[10] M. L. Gening, Y. E. Tsvetkov, G. B. Pier, N. E. Nifantiev, *Russ. J. Bioorg. Chem.* **2006**, *32*, 432–443.
[11] K. S. Kim, B.-Y. Lee, S. H. Yoon, H. J. Jeon, J. Y. Baek, K.-S. Jeong, *Org. Lett.* **2008**, *10*, 2373–2376.
[12] P. R. Ashton, C. L. Brown, S. Menzer, S. A. Nepogodiev, J. F. Stoddart, D. J. Williams, *Chem. Eur. J.* **1996**, *2*, 580–591.
[13] P. R. Ashton, S. J. Cantrill, G. Gattuso, S. Menzer, S. A. Nepogodiev, A. N. Shipway, J. F. Stoddart, D. J. Williams, *Chem. Eur. J.* **1997**, *3*, 1299–1314.
[14] G. Gattuso, S. Menzer, S. A. Nepogodiev, J. F. Stoddart, D. J. Williams, *Angew. Chem. Int. Ed. Engl.* **1997**, *36*, 1451–1454.
[15] S. A. Nepogodiev, G. Gattuso, J. F. Stoddart, *J. Inclusion Phenom. Mol. Recognit. Chem.* **1996**, *25*, 47–52.
[16] M. L. Gening, Y. E. Tsvetkov, G. B. Pier, N. E. Nifantiev, *Carbohydr. Res.* **2007**, *342*, 567–575.
[17] Y. Ohnishi, H. Ando, T. Kawai, Y. Nakahara, Y. Ito, *Carbohydr. Res.* **2000**, *328*, 263–276.
[18] U. Olsson, E. Sáwén, R. Stenutz, G. Widmalm, *Chem. Eur. J.* **2009**, *15*, 8886–8894.
[19] B. Mulloy, T. A. Frenkiel, D. B. Davies, *Carbohydr. Res.* **1988**, *184*, 39–46.
[20] R. Stenutz, I. Carmichael, G. Widmalm, A. S. Serianni, *J. Org. Chem.* **2002**, *67*, 949–958.
[21] C. H. Gotfredsen, A. Meissner, J. Ø. Duus, O. W. Sørensen, *Magn. Reson. Chem.* **2000**, *38*, 692–695.
[22] A. Meissner, O. W. Sørensen, *Magn. Reson. Chem.* **2001**, *39*, 49–52.
[23] A. A. Grachev, A. G. Gerbst, N. E. Ustyuzhanina, E. A. Khatuntseva, A. S. Shashkov, A. I. Usov, N. E. Nifantiev, *J. Carbohydr. Chem.* **2005**, *24*, 85–100.
[24] X. Zhu, R. R. Schmidt, *Angew. Chem. Int. Ed.* **2009**, *48*, 1900–1934.
[25] K. J. Najdoo, M. Kuttel, *J. Comput. Chem.* **2001**, *22*, 445–456.
[26] V. N. Viswanadhan, A. K. Ghose, G. R. Revankar, R. K. Robins, *J. Chem. Inf. Comput. Sci.* **1989**, *29*, 163–172.
[27] N. Cerca, K. K. Jefferson, T. Maira-Litran, D. B. Pier, C. Kelly-Quintos, D. A. Goldmann, J. Azeredo, G. B. Pier, *Infect. Immun.* **2007**, *75*, 3406–3413.
[28] D. Mack, W. Fischer, A. Krokotsch, K. Leopold, R. Hartmann, H. Egge, R. Laufs, *J. Bacteriol.* **1996**, *178*, 175–183.
[29] X. Wang, J. F. Preston, T. Romeo, *J. Bacteriol.* **2004**, *186*, 2724–2734.
[30] G. P. Sloan, C. F. Love, N. Sukurnar, M. Mishra, R. Deora, *J. Bacteriol.* **2007**, *189*, 8270–8276.
[31] E. A. Izano, I. Sadovskaya, E. Vinogradov, M. H. Mulks, K. Velllyagounder, C. Ragunath, W. B. Kher, N. Ramasubbu, S. Jabbouri, M. B. Perry, J. B. Kaplan, *Microb. Pathog.* **2007**, *43*, 1–9.
[32] Y. Itoh, X. Wang, B. J. Hinnebusch, J. F. Preston, T. Romeo, *J. Bacteriol.* **2005**, *187*, 382–387.
[33] T. Oguma, H. Kawamoto, *Trends Glycosci. Glycotechnol.* **2003**, *15*, 91–99.

Received: November 6, 2009
Published Online: March 17, 2010

